Iranian Journal of Organic Chemistry Vol. 12, No. 3 (2020) 2885-2898

IranJOC
Iranian Journal of Organic Chemistry

Symmetry breaking in the planar configurations of hydrazine, diphosphane and diarasane

Abdolkhalegh Mohammadizadeh[a] and Reza Fazaeli[*b]

[a]*Department of Chemistry, Arak Branch, Islamic Azad University, Arak, Iran*
[b]*Department of Chemistry, South Tehran Branch, Islamic Azad University, Tehran, Iran.*

Received: May 2020; Revised: June 2020; Accepted: July 2020

Abstract: If the excited and ground electronic modes are mixed, the symmetry breaking in the high symmetrical configuration of a molecule is expected. It has been shown that high-symmetry forms of any molecule undergo structural distortions due to the pseudo-Jahn-Teller Effect (PJTE). The planar (D_{2h}) and trans-bent (C_{2h}) geometries of Hydrazine (**1**), Diphosphane (**2**), and Diarsane (**3**) have been optimized at the CCSD(T), LC-PBE, CAM-B_3LYP and B_3LYP levels with 6-311+G** the basis set on every atom. Furthermore, studies have explored the associations between the PJT stabilization energies, hardness, and structural factors and applied NBO interpretation to study the mixing between the H_1–X_2 bonding and LPX_2 with X_3-H_5 anti-bonding configurations of **1**–**3** compounds. The energy gaps between the reference states)Δ (in the planar (D_{2h}) structures decrease from **1** to **3** compounds (3.80,3.12 and 2.77 eV). The plot of EPJT is linearly correlated with Δ [η (C_{2h})-η (D_{2h})] of compounds **1**–**3**. The calculated Δ[η (C_{2h})-η (D_{2h})] parameter increases from **1** to **3** compounds. It was shown that the planar (D_{2h})is more unstable than the trans-bent (C_{2h}) configuration, due to the strong lone pair–lone pair repulsion. PJT stabilization energy increases from compounds **1** to **3**, which represent greater stability of **1** to **3** compounds.

Keywords: Symmetry breaking, B_3LYP, Hydrazine, Diphosphane, Diarsane.

Introduction

It has been shown that the various compounds become more stable to undergo structural distortions [1-3]. The pseudo-Jahn-Teller Effect (PJTE) is the stabilization process, which happens when two or more electron states are mixed that are approximately degenerate due to a special asymmetric distortion [4-5]. If the excited and ground electronic modes are mixed together, the symmetry breaking in the high symmetrical geometry of a structure is expected. [6]. It has been shown that high-symmetry forms of any molecule undergo structural distortions due to the JTE [7-10].Yang Liu et al. (2015) conducted a study to investigate the PJTE in Tetrasilacyclobutadiene Analogues.

The geometry Si_4R_4 or Ge_4R_4 analogs are optimized by the DFT with the B_3LYP functional. Electronically excited states and potential energy profiles along with different vibrational modes are gathered with the CASSCF method [11-12]. In the investigation of the effect of PJTE on the Si_4R_4 molecule (D_{4h} symmetry), two typical equilibrium structures were obtained due to the symmetry breaking [13]. They began with Si_4F_4 and Ge_4F_4 molecules to justify the basis of boat-like and chair-like configurations of Si_4R_4 analogs. Along b_{2u}, the D_{4h} configuration in 1^1B_{2g} is not stable and undergoes distortions naturally up to the lowest point at Q = 0.7A having the boat-like configuration. It is not easy to analyze the likely distortions alongwithb_{1g} andb_{2g}. Along b_{1g} Mixing of ground state 1^1A_{1g} and exited states 1^1B_{1g}and2^1A_{1g} and along with b_{2g} Mixing of ground state1^1Ag and exited states ^1B_2gand1^1Agtake

*Corresponding author. Tel.:+989128595684; E-mail: r_fazaeli@azad.ac.ir

place. Comparing the bonding feature and LUMO-HOMO gaps in Si_4R_4 and Ge_4R_4 indicates that the Ge_4R_4 compounds are expectedly steadier in the chair-like configurations than the matching Si_4R_4 analogs. In 2015, Yang Liu et al. Studied PJTE in deformation of the flat configuration of tetra-heterocyclic 1,2-diazetes $C_2N_2E_4$, E = H, F, Cl, Br[14]. There are eighteen degrees of freedom vibration in eight-atom systems $C_2N_2E_4$.Two imaginary frequencies have been detected in all these computations: the first one is a_2 type and the other one is b1. The first one has a C_2 configuration, while the second has a Cs symmetry and higher than the first one by 5–8 kcal/mol. Ayan et al. investigated PJTE for C6S8 and its suppression in S-oxygenated dithiine ($C_4H_4(SO_2)_2$)[15]. In the gas-phase, the tricyclic carbon-sulfide, C_6S_8 molecule has a 'butterfly flapping' kind distorted ground state and in β-phase of the crystal. It is possible to track the basis of the distortion causing reduced symmetry from C_2h to C_2 by a (1Ag + 1Au + 2Au + 3Au) ⊗ au pseudo Jahn–Teller effect (PJTE) problem. The S-oxygenated derivative of dithiine, contrary to the other dithiines, C_4H_4 $(SO_2)_2$ (2) stays flat. Unlike the C6S8, where the energy gap between the ground and its excited state (Δ) is equal to 2.85 eV, this difference is high in the C_4H_4 $(SO_4)_2$ composition and is equal to 6.55 eV. Also vibronic coupling (F0i) for $C_4H_4(SO_2)_2$ is much lower than C6S8. As these calculations show, the PJT effect is a method to explain the distortion of molecular.

By the Neutron diffraction investigations showed that normal hydrogen and bifurcated bindings are too common in many hydrazinium salts [16-17]. The reduction in the bond longitude in N_2H_5 correlated to N_2H_4 is referred to as the decrease of the electron cloud repulsion on nitrogen atoms.

Various computations have been carried out on the molecular and electronic configurations of the parent compounds (PH)n with n = 3-6. The results of these computations show that the five-membered ring in (PH) 5 possesses either a rather distorted envelope form (C1symmetry) or asymmetrical envelope conformation (Cs symmetry). $(PH)_5$ outperforms $(PH)_3$, $(PH)_4$, as well as P_2H_4 and P_3H_5 in terms of stability[18-20]. The HAsAsH molecule has hitherto only been proposed tentatively as a short-lived species generated in electrochemical or microwave-plasma experiments. M. Gardner et al. reported Isolation of Elusive HAsAsH in a Crystalline Diuranium(IV) Complex [21].

Characterization and computational data are consistent with back-bonding-type interactions from uranium to the HAsAsH Π*-orbital. HNNH is just detected in the solid case when connected to metals [22]. The valence shell electron pair repulsion (VSEPR) theory[23-24] has clearly identified the lone pair–lone pair repulsion; according to this theory, the lone pair–lone pair repulsion is more powerful than a lone pair-bonding pair repulsion; which can be exemplified through hydrazine (H2N–NH2) in three dissimilar conformations (cis, trans, and skew) [25]. The trans conformer will have the greatest stability by quenching the influence of the hyper-conjugation. According to the natural bond orbital (NBO) analysis, the N–N bond has two different hybridization mode, sp3.56 in trans versus sp3.12 in cis conformer [26-27]. Although much the information has been published on the structures of Hydrazine (**1**), Diphosphane (**2**), and Diarsane (**3**) derivatives, information about the basis of the symmetry breaking in these compounds (from planar to trans-bent) and comparison with the pseudo-Jahn–Teller effect has not been published yet.

Results and discussion

The associations between the PJTparameters of Hydrazine (**1**), Diphosphane (**2**) and Diarsane (**3**) and NBO analysis have been investigated through TD-DFT[28] in the current research. It has been shown that a mixture of the excited and ground electronic wave functions under the $D_2h \rightarrow C_2h$ distortions will distort the high-symmetric (D_{2h}) configurations of **1–3** compounds because of the vibronic coupling (i.e. PJTE). The mixing of the excited and ground electronic states also lead to symmetry break up in the high symmetrical configuration of compounds [7].

When a high-symmetric compound does not have the PJTE in the Q direction, the force constant (K_0) is defined as follows:

$$K_0 = \langle \Psi_1 \left| \left(\frac{\partial^2 H}{\partial Q^2} \right)_0 \right| \Psi_1 \rangle \qquad (1)$$

Where H is the Hamiltonian. When the force constant with no PJTE is positive ,$K_0 > 0$.It is possible to mix the ground and excited state under Q to show the decreased force constant, $K=K_0 - (F^2/\Delta)$ (F and Δ represent vibronic coupling and the energy difference between the two states, respectively). If coupling constant,

$$F = \langle \Psi_1 \left| \left(\frac{\partial H}{\partial Q} \right)_0 \right| \Psi_2 \rangle \qquad (2)$$

If $(F^2/\Delta) > K_0$ then $K < 0$.In this case, the system in the direction of Q is not stable.

Moreover, the D_{2h} and C_{2h} geometries of **1**–**3** molecules were optimized at the CCSD(T), LC-PBE, CAM-B3LYP and B3LYP levels with 6-311+G** the basis set on any atoms. Besides, studies have explored the associations between the PJT stabilization energies, hardness, and structural factors and applied NBO analyses [29] to justify the mixing between the H_1–X_2 bonding and LPX_2 with X_3-H_5 anti-bonding configurations of **1**–**3** molecules.

1-Planar and trans-bent interconversions

Table **1** shows the B_3LYP/6-311+G**, CAM-B_3LYP/6-311+G**, LC-ωPBE/6-31+G** and CCSD (T)/6-311+G** corrected electronic energy ($E_0 = E_{el}$ + ZPE) differences between the trans-bent (C_{2h}) and planar (D_{2h}) configuration of **1**–**3** compounds.

Our results have been showing that the given barrier peak for the $C_{2h} \rightarrow C_{2h'}$ through their matching planar (D_{2h}) forms increased from **1** to **3** compounds (Figure **1**).

CCSDT/6-311+G**

ΔE_0^a { 1=25.93; 2=82.24; 3=92.83

LC-ωPBE/6-311+G**

ΔE_0^a { 1=18.61; 2=73.91; 3=88.09

CAM-B_3LYP/6-311+G**

ΔE_0^a { 1=19.51; 2=76.62; 3=91.56

B_3LYP/6-311+G**

ΔE_0^a { 1=20.93; 2=78.14; 3=93.84

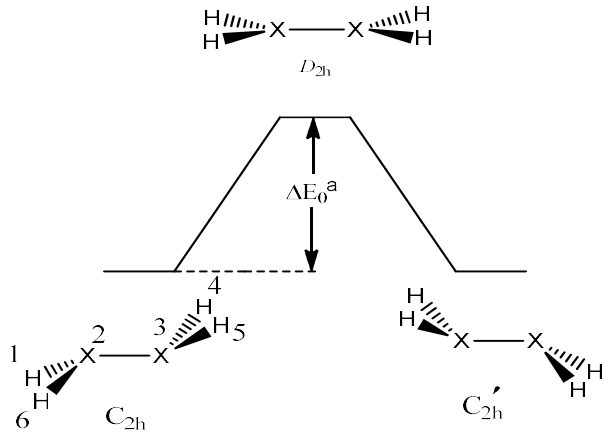

X=N,P,As

Figure 1: Calculated energy profiles of the trans-bent configuration interconversions of compounds **1–3** via their Corresponding planar forms$[C_{2h}] \rightarrow [D_{2h}]^{\neq} \rightarrow [C_{2h}']$.

For the instability of a high symmetrical polyatomic system, it is necessary to have some electronic states that interact powerfully with each other. [7-10]. The normal modes of the D_{2h} structure of **1**–**3** compounds that direct them to C_{2h} structure, It has a b_{2g} symmetry. Studies have shown that the imaginary vibrational frequencies of D_{2h}structure of **1**–**3** compounds are 1024.8i, 1010.3i, and 1027.9i cm^{-1}, respectively, These frequencies were obtained through B3LYP/6-311+G** level. Our results show that global hardness difference improved from compound **1** to compound **3**.

The PJTE has caused the mixing of the excited B_2g and ground Ag states which is related to the mixing of and orbitals in **1–3** compounds. Due to this mixing a distortion occurs from D_{2h} to C_{2h}) structures of **1–3** compounds (Figure **2**).

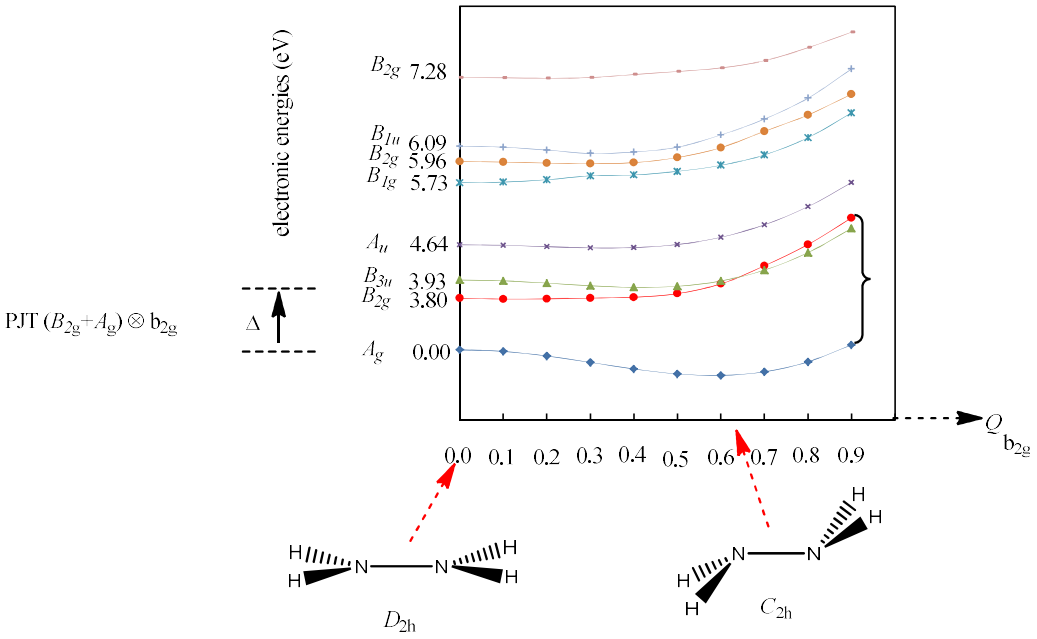

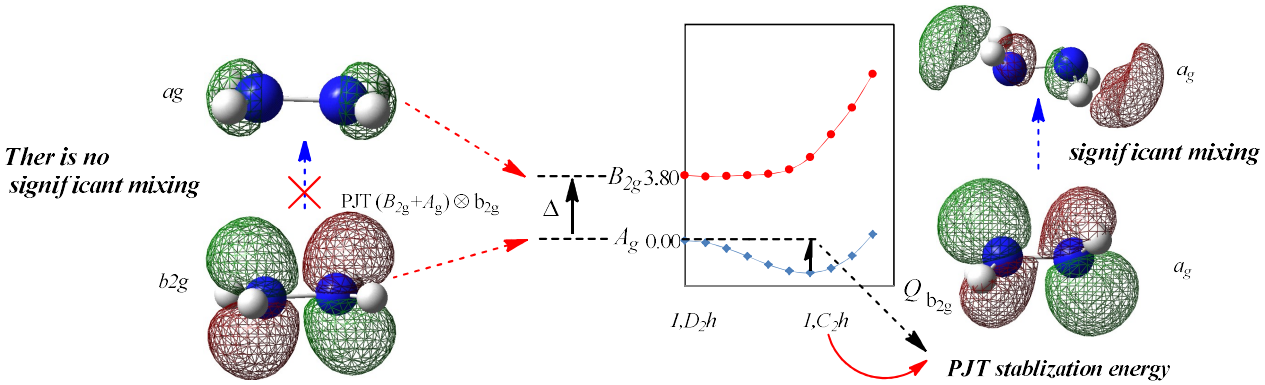

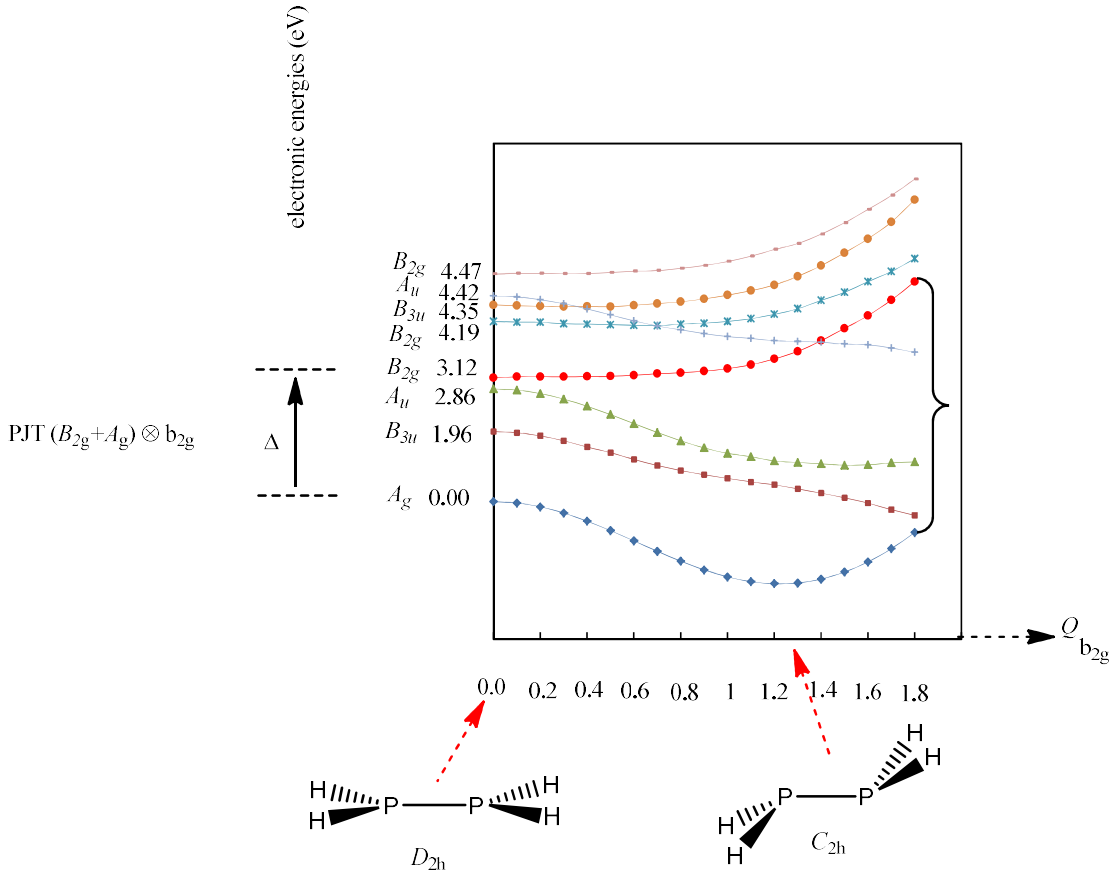
electronic energies (eV)
PJT (B_{2g}+A_g) ⊗ b_{2g}
Δ
B_{2g} 4.47
A_u 4.42
B_{3u} 4.35
B_{2g} 4.19
B_{2g} 3.12
A_u 2.86
B_{3u} 1.96
A_g 0.00
$Q_{b_{2g}}$
0.0 0.2 0.4 0.6 0.8 1 1.2 1.4 1.6 1.8
D_{2h}
C_{2h}

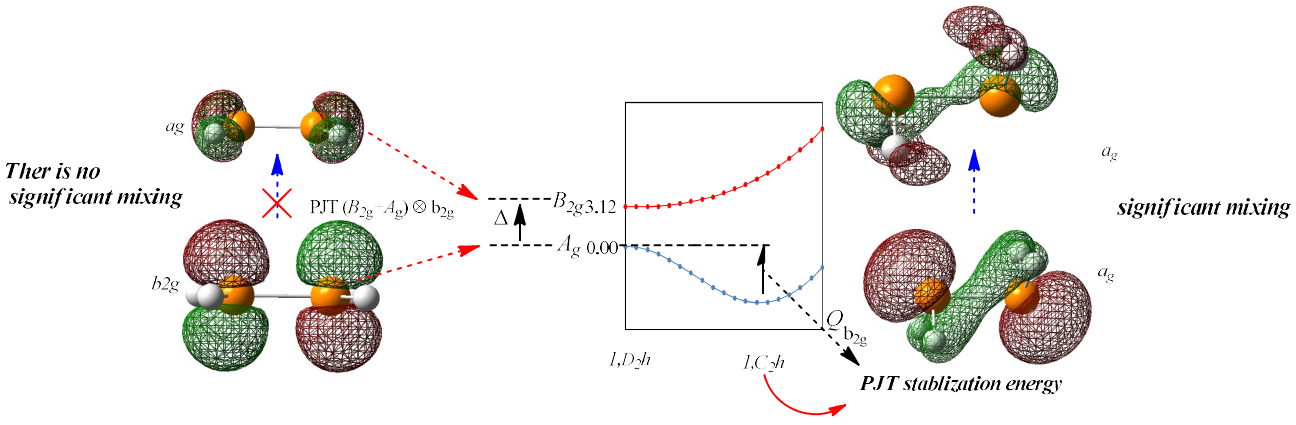
ag
Ther is no
significant mixing
PJT (B_{2g}–A_g) ⊗ b_{2g}
b2g
Δ
B_{2g}3.12
A_g 0.00
$Q_{b_{2g}}$
1,D2h
1,C2h
PJT stablization energy
a_g
significant mixing
a_g

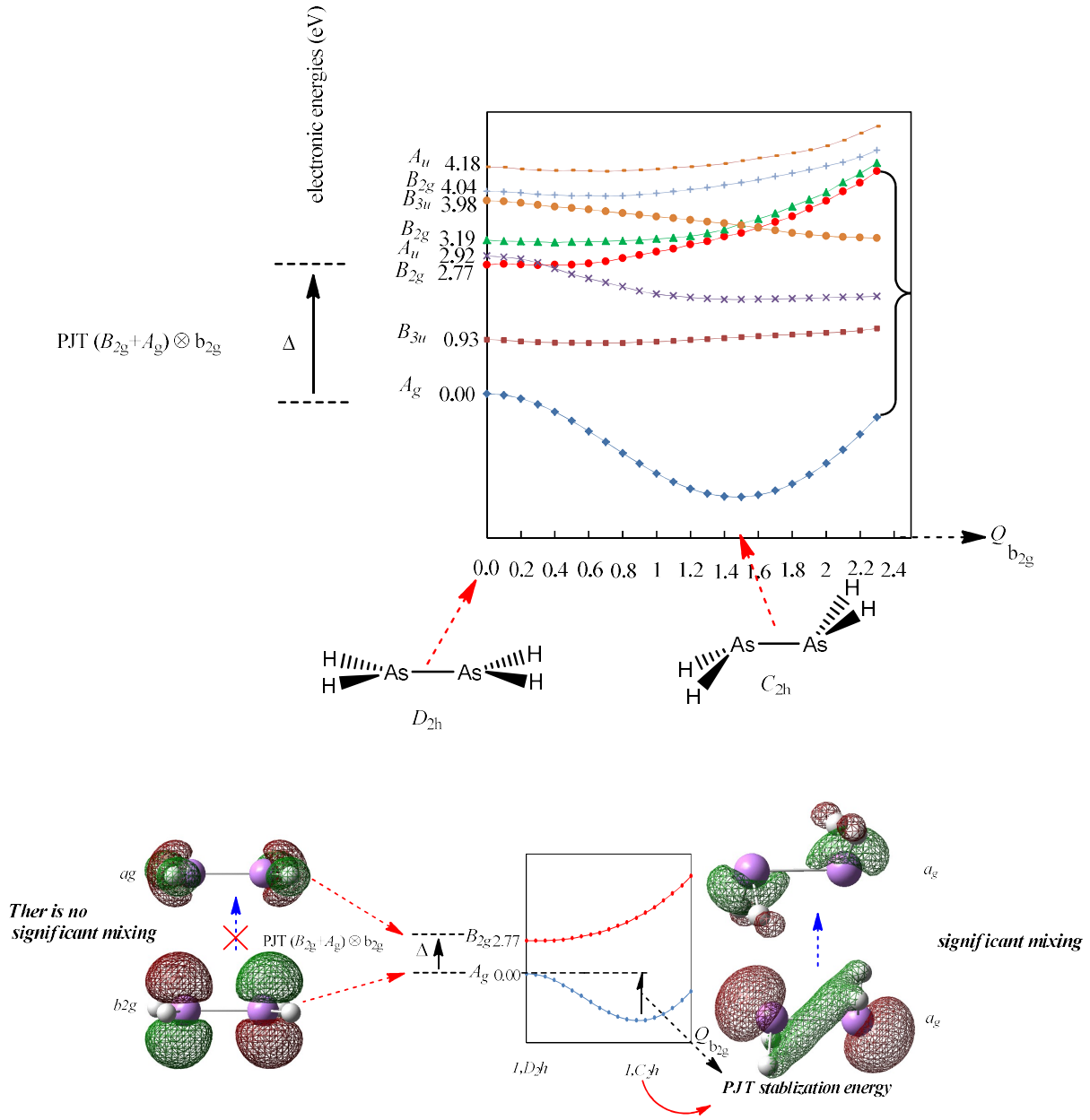

Figure 2: TD-DFT (B3LYP/6-311+G**) energy curves (in eV) of the ground and excited states in the bending directions of **1–3** compounds.

The energy curves of the states with their changes during the distortion mode [Q_{b2g}] have been showing in Fig.2. As to be seen, PJT stabilization energy raises from 1 to 3 compounds, which represents greater stability of compound **1** to **3** (0.4, 1.35and 1.77 eV). The energy gaps)Δ (between D_{2h} structures decrease from **1** to **3** compounds (3.80, 3.12, and 2.7 eV). It was predicted that PJT stabilization energy would be increased and Δ would be reduced. The stability of the compounds is increased from **1-3** compounds for D_{2h} → C_{2h}.

The presence of only one, two, or more excited states was effective to soften the ground-state structures that have high-symmetry. The valence of **1−3** compounds are isoelectronic, thus, they may be similar in terms of vibronic coupling constant values (F). Based on equation 3, it is possible to decrease the force constant (i.e., K) along with the $Q_{(b2g)}$ from **1 - 3** compounds following the reduction in the energy interval between the excited and ground states interaction (Δ) [30].

$$K = K_0 - \left(\frac{F^2}{\Delta}\right) \qquad (3)$$

2-Geometricparameters

The geometric parametersof the D_{2h} and C_{2h}symmetry of **1-3** compounds as calculated at the B_3LYP/6-311+G**, CAM- B_3LYP/6-311+G**, LC-ωPBE/6-31+G**and CCSD(T)/6-311+G** levels of theory are shown in table **2**. Our results showed the flap angles between the H_2X Plaines and the X→X bonds in the bend form (C_{2h}) increase from **1 to 3**compounds (Figure **3**).

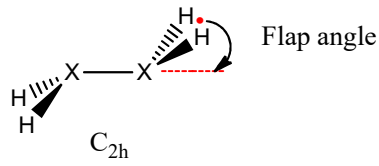

Figure 3: flap angle in the C_{2h} structure of compounds **1-3** (X=N, P, As)

According to all Four levels of theory, the difference in bond longitudebetween the X→X bonds in the D_{2h} and C_{2h}configurations were calculated(i.e.Δ[rx-x(C2h)-rx-x(D2h)]), whichincrease from **1** to **3** compounds (see Table **2**). Note that EPJT is linearly correlated versusΔ[rx-x(C2h)-rx-x(D2h)] in compounds **1–3** (Figure **4**).

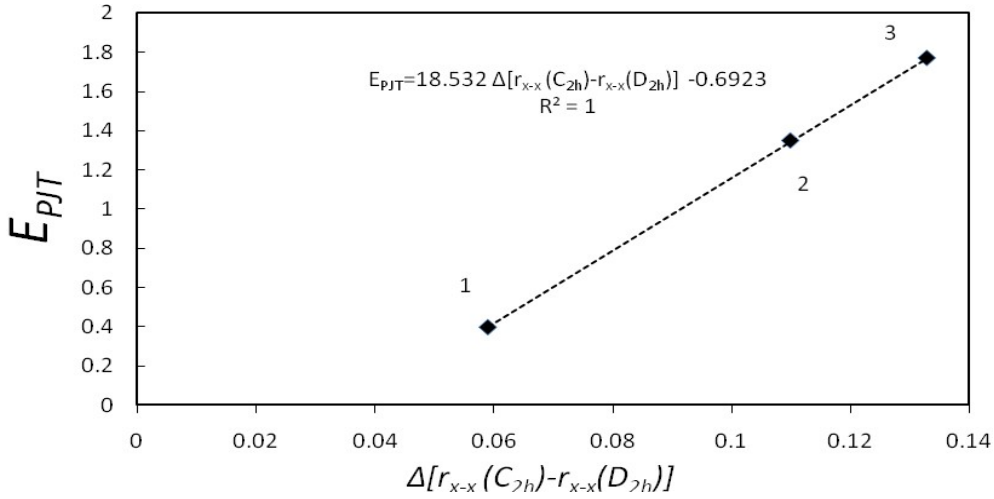

Figure 4: EPJT(eV) versus Δ[rx-x (C_{2h})-rx-x(D_{2h}) Parameters for compounds **1-3** showing an excellent linear Correlation

The increase of the [rx-x(C2h)-rx-x(D2h)] parameter is parallel to the increase of the EPJT ongoing from **1** to **3** compounds. Consequently, the Δ[rx-x(C2h)-rx-x(D2h)] parameter could be a criterion to assess the EPJT in compounds **1–3**.

3-Global Hardness

Table **3** shows the energies of LUMO and HOMO of the D2h and C2h structures of **1–3** compounds, as calculated at the LC ωPBE/6-31+G** level. The energy difference between the HOMO and LUMO was reduced from the D2h and C2h configuration of **1** to **3** compounds. The relationship between the global hardness (η), ionization potential (I) and electron affinity (A) of a molecule is indicated by the following equation:

$$\eta = o.5\,[I - A] \qquad (5)$$

The hardness (η) can be written by the Koopmans 'theory by the following expression:

$$\eta = 0.5(E_{LUMO} - E_{HOMO})$$

As shown in Table **3**, variations between the global hardness in the D_{2h} and C_{2h} structures (Δ [η (C_{2h})-η (D_{2h})]) increase from compound **1** to **3**compounds. As shows in Figure **5**, the plot of E_{PJT} is linearly correlated with Δ [η (C_{2h})-η (D_{2h})] of compounds **1**–**3**. The calculatedΔ[η (C_{2h})-η (D_{2h})] parameter

increases from **1** to **3**. Consequently, the variations of the barrier peaks for the $C_{2h} \rightarrow C_{2h}'$ interconversion processes [i.e. $C_{2h} \rightarrow (D_{2h})^{\neq} \rightarrow C_{2h}'$] from **1** to **3**compounds can be used to justify the variations of $\Delta[\eta\,(C_{2h})\text{-}\eta\,(D_{2h})]$ parameters.

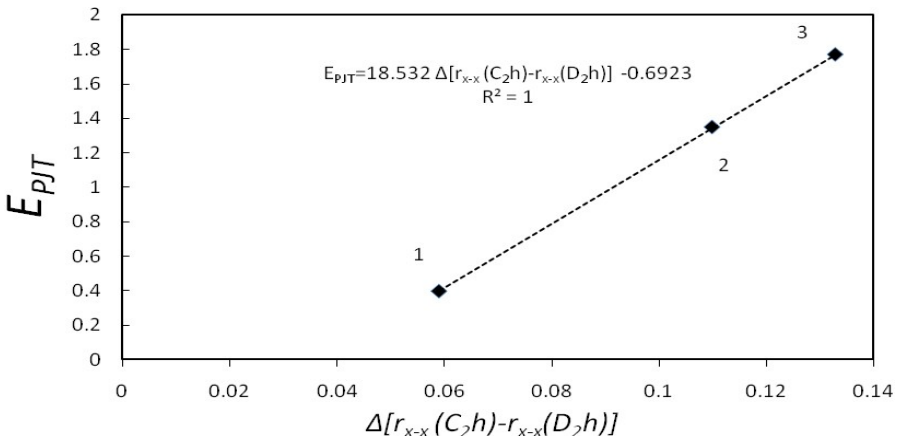

Figure 5: Fit EPJT(eV) versus $\Delta[\eta\,(C_{2h})\text{-}\eta\,(D_{2h})]$of compound 1-3 showing an excellent linear correlation

4-Stabilization energies related to the electron delocalizations

Figure **1** and **2** have been show the PJT stabilization energies (E_2), which increase from **1** to **3** compounds. The EPJT is brought about following the mixing of the ground ($A_{g)}$ and excited ($B_{2g)}$ electronic states related to the mixing of the $^{\Psi}$HOMO (b_{2g}) and the $^{\Psi}$LUMO+1 (A_g). Note that the symmetry of mixing orbitals to $a_g$by PJT distortions in the planar structures of **1**–**3**($D_{2h} \rightarrow C_{2h}$) along with b_{2g} displacement. The results of NBO (Table **4**) indicate that NBO5 and nboview (Figure **6**) explored the stability of the trans-C_{2h} against D_{2h} structures of **1**–**3**.

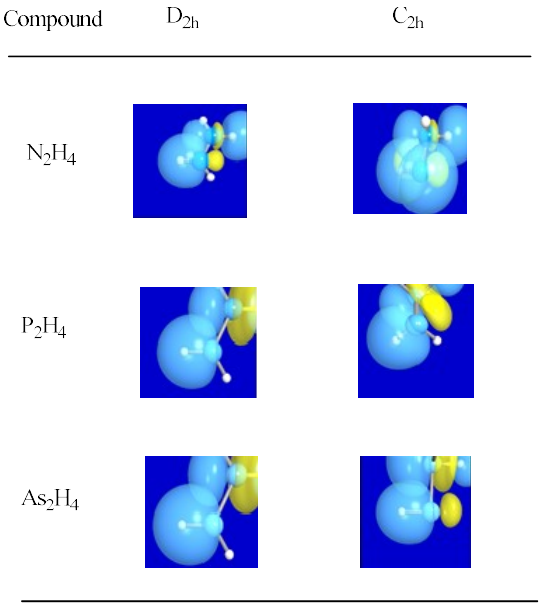

Figure 6: NBO plot mixing donor orbitals ($\sigma_{H1\text{-}X2}$ و LP_{X2}) and acceptor orbital ($\sigma^*_{X3\text{-}H5}$)

The results obtained from(E_2), donor orbitals ($\sigma_{H1\text{-}X2}$andLP_{X2}) and acceptor orbitals ($\sigma^*_{X3\text{-}H5}$) calculations have been shown that the C_{2h} configurations of **1**compounds outperform their corresponding D_{2h} configuration in terms of stability, but thegreater stability of the C_{2h}against D_{2h}configurations of **2**–**3** compounds is not justified.

5-Lone pair-Lone pair repulsion

The **VSEPR** theory [23-24] identifies the Lp–Lprepulsion clearly; according to this theory, the Lp–Lprepulsion is more powerful than Lp–bonding pair repulsion. The position of lone pairs (red lines) are shown in fig.7.Using NBO and Pairwise steric exchange energy calculations, It was shown that the planar (D_{2h})is more unstable than trans-bent (C_{2h}) configuration, due to the strong lone pair–lone pair repulsion (Calculation results shown in Table **5**)

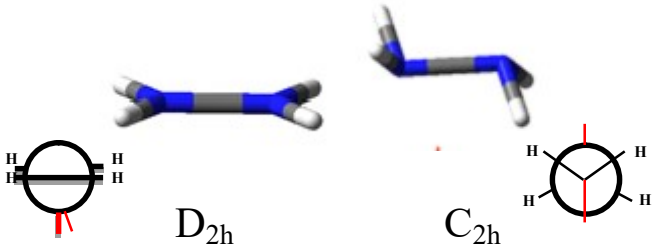

Figure 7: Comparison of two conformations of 1-3 compounds computed at the B3LYP/6-311+G** level. The red lines represent the X lone pairs

Conclusion

To enhance the D_{2h} and C_{2h}structures of **1**–**3** compounds, B_3LYP/6-311+G**, CAM- B3LYP/6-311+G**, LC-ωPBE/6-31+G**and CCSD (T)/6-311+G** levels were applied. Calculations have explored the associations between the PJT stabilization energies(E_2), hardness, and structural factors. Some imaginary frequencies have been applied to specify the character of the stationary points of the excited and ground states for **1-3** compounds. TD-DFT was applied to investigate of the $C_{2h}$and D_{2h}structures of **1**–**3**. TD-DFT methodology was applied to investigate the electronic configurations of the D_{2h} and C_{2h}symmetry of **1**–**3** structures. NBO calculations with NBO5 and NBOVIEW programs were performed at the B3LYP/6-311+G**level to investigated all structures of **1**–**3**.

The PJTE has caused the mixing of the excited B_2g and ground Ag states which are related to the mixing of $\Psi_{Homo}(b_{2g})$ and $\Psi_{Lumo+1}(a_g)$ orbitals in **1**–**3** compounds. Due to this mixing ($PJT(A_g + B_{2g}) \otimes b_{2g}$) a distortion occurs from D_{2h} to C_{2h}) structures of **1**–**3** compounds. Variations between the global hardness in the $D_{2h}$and C_{2h} structures (i.e. Δ [η (C_{2h})-η (D_{2h})]) an increase from **1-3**. The results E_2, donor orbitals($\sigma H_1\text{-}X_2$andLPX)and acceptor orbitals($\sigma^*X_3\text{-}H_5$) calculations showed that the C_{2h} configurations of compound **1** outperform their corresponding planar (D_{2h}) configuration in terms of stability, but the greater stability of the trans-bent (C_{2h}) against (D_{2h}) configurations of compounds **2**–**3** is not justified. It was shown that the $D_{2h}$is more unstable than C_{2h}configuration; due to the strong lone pair–lone pair repulsion.

Table 1. CCSD(T)/6-311+G**, LC-ωPBE/6-311+G**, CAM-B3LYP/6-311+G** and B3LYP/6-311+G** calculated correctedelectronic energies (in kcal/mol) (E_o=E_{el}+ZPE for the planar (D_{2h}) and trans-bent (C_{2h}) geometries of compounds **1-3**.

Method	B3LYP/6-311+G**,			CAM-B3LYP/6-311+G**,			LC-ωPBE/6-311+G**			CCSD(T)/6-311+G**,	
	ZPE[b]	E_0	ΔE_0^a	*ZPE*	E_0	ΔE_0^a	*ZPE*	E_0	ΔE_0^a	E_0	ΔE_0^a
compound											
1, C_{2h}	0.052545	-111.852982	0.00	0.053132	-111.797854	0.00	0.053737	-111.782839	0.00	-111.569942	0.00
1, D_{2h}	0.049549	-111.819626	20.93	0.049891	-111.766751	19.51	0.050293	-111.753178	18.61	-111.528612	25.93
2, C_{2h}	0.034835	-685.119014	0.00	0.035572	-685.083231	0.00	0.363050	-684.863089	0.00	-684.068956	0.00
2, D_{2h}	0.032237	-684.994485	78.14	0.032706	-684.961120	76.62	0.033203	-684.745295	73.91	-683.937888	82.24
3, C_{2h}	0.031260	-4474.139718	0.00	0.031924	-4474.287130	0.00	0.032755	-4473.443532	0.00	-4470.90624	0.00
3, D_{2h}	0.028657	-4473.990161	93.84	0.029317	-4474.141208	91.56	0.029965	-4473.303139	88.09	-4470.754695	92.83

Table 2: Calculated geometric parameters of the D_{2h} symmetry and C_{2h} configurations of **1-3** compounds.

Compound	**1**		**2**		**3**	
Geometry	D_{2h}	C_{2h}	D_{2h}	C_{2h}	D_{2h}	C_{2h}
Bond lengths (Å)						
r_{X-X}	(1.421)[a]	(1.480)[a]	(2.163)[a]	(2.273)[a]	(2.362)[a]	(2.495)[a]
	(1.408)[b]	(1.451)[b]	(2.138)[b]	(2.214)[b]	(2.319)[b]	(2.419)[b]
	(1.421)[c]	(1.480)[c]	(2.163)[c]	(2.273)[c]	(2.362)[c]	(2.495)[c]
	(1.415)[d]	(1.465)[d]	(2.151)[d]	(2.245)[d]	(2.342)[d]	(2.460)[d]
r_{X-H}	(0.997)[a]	(1.018)[a]	(1.384)[a]	(1.424)[a]	(1.471)[a]	(1.524)[a]
	(0.996)[b]	(1.014)[b]	(1.381)[b]	(1.414)[b]	(1.459)[b]	(1.510)[b]
	(0.997)[c]	(1.018)[c]	(1.384)[c]	(1.424)[c]	(1.471)[c]	(1.527)[c]
	(0.997)[d]	(1.016)[d]	(1.381)[d]	(1.418)[d]	(1.464)[d]	(1.518)[d]

$\Delta[r_{X\text{-}X}\ (C_{2h})\text{-}\ r_{X\text{-}X}\ (D_{2h})]^a$	0.059		0.110		0.133	
$\Delta[r_{X\text{-}X}(C_{2h})\text{-}\ r_{X\text{-}X}\ (D_{2h})]^b$	0.043		0.076		0.100	
$\Delta[r_{X\text{-}X}\ (C_{2h})\text{-}\ r_{X\text{-}X}\ (D_{2h})]^c$	0.059		0.110		0.133	
$\Delta[r_{X\text{-}X}(C_{2h})\text{-}\ r_{X\text{-}X}\ (D_{2h})]^d$	0.050		0.094		0.118	
Bond angles (°)						
$\theta_{H\text{-}X\text{-}X}$	$(118.6)^a$	$(104.5)^a$	$(118.9)^a$	$(93.9)^a$	$(118.7)^a$	$(92.1)^a$
	$(118.7)^b$	$(105.5)^b$	$(118.7)^b$	$(97.7)^b$	$(118.6)^b$	$(92.7)^b$
	$(118.6)^c$	$(104.5)^c$	$(118.9)^c$	$(93.9)^c$	$(118.7)^c$	$(92.1)^c$
	$(118.6)^d$	$(105.1)^d$	$(118.8)^d$	$(94.3)^d$	$(118.6)^d$	$(92.4)^d$
$\theta_{H\text{-}X\text{-}H}$	$(122.7)^a$	$(103.3)^a$	$(122.1)^a$	$(92.4)^a$	$(122.5)^a$	$(91.2)^a$
	$(122.4)^b$	$(103.7)^b$	$(122.4)^b$	$(92.9)^b$	$(122.7)^b$	$(91.9)^b$
	$(122.7)^c$	$(103.3)^c$	$(122.1)^c$	$(92.4)^c$	$(122.5)^c$	$(91.2)^c$
	$(122.6)^d$	$(103.7)^d$	$(122.2)^d$	$(92.7)^d$	$(122.6)^d$	$(91.6)^d$
Torsion angles (°)						
$\theta_{H1\text{-}X\text{-}X\text{-}H4}$	$(0.0)^a$	$(71.7)^a$	$(0.0)^a$	$(87.2)^a$	$(0.0)^a$	$(88.6)^a$
	$(0.0)^b$	$(70.5)^b$	$(0.0)^b$	$(86.6)^b$	$(0.0)^b$	$(87.6)^b$
	$(0.0)^c$	$(71.7)^c$	$(0.0)^c$	$(87.2)^c$	$(0.0)^c$	$(88.6)^c$
	$(0.0)^d$	$(70.81)^d$	$(0.0)^d$	$(86.8)^d$	$(0.0)^d$	$(88.2)^d$
				$(61.0)^f$		
Flap Angles (°)						
	$(0.0)^a$	$(66.1)^a$	$(0.0)^a$	$(84.2)^a$	$(0.0)^a$	$(87.0)^a$
	$(0.0)^b$	$(64.2)^b$	$(0.0)^b$	$(83.1)^b$	$(0.0)^b$	$(86.0)^b$
	$(0.0)^c$	$(66.1)^c$	$(0.0)^c$	$(84.2)^c$	$(0.0)^c$	$(87.0)^c$
	$(0.0)^d$	$(64.9)^d$	$(0.0)^d$	$(86.6)^d$	$(0.0)^d$	$(86.4)^d$

[a] From CCSD(T)/6-311+G**, [this work]. [b] From LC-ωPBE/6-311+G**, [this work].
[c] From B3LYP/6-311+G**, [this work]. [d] From CAM-B3LYP/6-311+G**, [this work]

Table 3: LC-wPBE/6-311+G** calculated energies (in hartree) of HOMO (ε_{HOMO}), LUMO (ε_{LUMO}), ε_{LUMO}-ε_{HOMO}, global hardness (η)and $\Delta[\eta$ (C_{2h})- η (D_{2h})] parameters for the C_{2h} and D_{2h} structures of **1-3** compounds.

compound	ε HOMO	ε LUMO	ε LUMO - ε HOMO	*I*	*A*	η	χ	$\Delta[\eta$ (C2h)-η (D2h)]
1, C_{2h}	-0.32310	0.10291	0.42601	0.32310	-0.10291	0.21300	0.11009	0.02578 (16.17)[a]
1, D_{2h}	-0.26382	0.11063	0.37445	0.26382	-0.11063	0.18722	0.07659	0.00000
2, C_{2h}	-0.34416	0.04820	0.39236	0.34416	-0.04820	0.19618	0.14798	0.04993 (31.33)[a]
2, D_{2h}	-0.25967	0.03283	0.29250	0.25967	-0.03283	0.14625	0.11342	0.00000
3, C_{2h}	-0.34179	0.03209	0.37388	0.34179	-0.03209	0.18694	0.15485	0.05745 (36.05)[a]
3, D_{2h}	-0.25330	0.00568	0.25898	0.25330	-0.00568	0.12949	0.12381	0.00000

Table 4: NBO-B3LYP/6-311+G**calculated stabilization energies(E_2, in kcal /mol) associated with electron delocalizations

compound	**1**		**2**		**3**	
geometry	D_{2h}	C_{2h}	D_{2h}	C_{2h}	D_{2h}	C_{2h}
E_2						
$\sigma_{H1-X2} \rightarrow \sigma^*_{X3-H5}$	2.06	1.78	1.20	1.10	1.14	0.84
$LP_{X2} \rightarrow \sigma^*_{X3-H5}$	0.0	0.58	0.0	0.0	0.0	0.0
ΣE_2	2.06	2.36	1.20	1.10	1.14	0.84

Table5: NBO-B3LYP/6-311+G**calculated pairwise steric exchange energy (in kcal /mol)for comparison of LP_x – LP_x repulsion effect

compound	D_{2h}	C_{2h}
$\mathbf{N_2H_4}$	36.15	17.68
$\mathbf{P_2H_4}$	17.69	12.32
$\mathbf{As_2H_4}$	13.73	1.19

References and notes

[1] Vafaei-Nezhad, M; Ghiasi, R; Shafiei, F, Russ. *Phys. Chem. A* **2020**, *94*, 772–777.
[2] Milani, N. N.; Ghiasi, R.; Forghaniha, A, *J. Appl. Spect.* **2020**, *86*, 1123-1131.
[3] Hajhoseinzadeh, K.; Ghiasi, R.; Marjani, A. *Eurasian Chem. Comm.* **2020**, *2*, 78-86.
[4] Salem, L. *The Molecular Orbital Theory of Conjugated Systems,* Benjamin/New York, **1966**.
[5] Pearson, R. G. *Symmetry Rules for Chemical Reactions,* Wiley/New York, **1976**.
[6] Bersuker, I. B. *The Jahn–Teller Effect*, Cambridge University Press/New York, **2006**.
[7] Bersuker, I. B. *Chem. Rev.* **2001**, *4*, 1067–1114.
[8] Bersuker, I. B. *The Jahn–Teller Effect,* Cambridge University /New York, **2006**.
[9] Bersuker, I. B. *Chem. Rev.* **2013**, *113*, 3, 1351–1390.
[10] Bersuker, I. B. *Phys. Rev. Lett.* **2012**, *108*, 137-202.
[11] Knowles, P. J.; Werner, H.-J, *Chem. Phys. Lett.* **1985**, *115*, 259–267.
[12] Werner, H.-J.; Knowles, P. J. A, *J. Chem. Phys.* **1985**, *82*, 5053–5063.
[13] Liu, Y.; Wang Y.; Isaac B. Bersuker, *Sci. Rep*. **2016**, *6*, 23315.
[14] Ilkhani, A. R.; Gorinchoy, N. N.; Bersuker, I. B. *Chem. Phys.*. **2015**, *460*, 106–110.
[15] Saied M. D.; Pratik, Ch.; Chowdhury, R.; Bhattacharjee, S. K.; Jahiruddin, A. D. *Chem. Phys.* **2015**, *460*, 101–105.
[16] Schmidt, E.W. *Hydrazine and its Derivatives: Preparation, Properties, Applications,* Wiley/New York, **2001**.
[17] Govindarajan, S. *Structural and thermal studies on hydrazinium (1+) metal sulfate and oxalate complexes. (Ph.DThesis*, Indian Institute of Science/ Bangalore 1938.
[18] Yoshifuji, M.; Inamoto, N.; Ito, K.; Nagase, S. *Chem. Lett,* **1985**, *14*, 437-440.
[19] Schoeller, W.; Staemmler, V.; Rademacher, P. *Inorg. Chem.* **1986**, *25*, 4382–4385.
[20] Schiffer, H.; Ahlrichs, R.; Häser, M. *Theor. Chim. Acta.* **1989**, *75*, 1-10.
[21] Gardner, B. M.; Bal. Z. S.; Scheer, M. Wooles, A. J.; Tuna, F.; McInnes, E. J. L.; McMaster, J.; Lewis, W.; Blake, A. J.; Liddle, S. T. *Angew Chem.* **2015**, *127*, 15465 –15469.
[22] Evans, W. J.; Kociok-Koehn, G.; Leong, V. S.; Ziller, J. W. *Inorg. Chem.* **1992**, *31*, 17, 3592–3600.

[23] Gillespie R. J.; Nyholm, R. S. Q. *Rev. Chem. Soc.* **1957**, 11, 339–380.
[24] Gillespie, R. J. *Coord. Chem. Rev*. **2008**, *252*, 1315–1327.
[25] Zhang, H.; Jiang, X.; Wu, W.; Mo, Y. *Phys. Chem. Chem. Phys.* **2016**, *18*, 11821-11828.
[26] Reed, A. E.; Curtiss L. A.; Weinhold, F. *Chem. Rev.* **1988**, *88*, 899–926.
[27] Weinhold F.; Landis, C. *Valency and Bonding,* Cambridge University Press, Cambridge/ England, **2005**.
[28] Runge E. Gross, E. K. U.*, Phys. Rev. Lett.* **1984**, *52*, 997-1000.
[29] Glendening, E. D.; Badenhoop, J. K.; Reed, A. E.; Carpenter, J. E.; Bohmann, J. A.; Morales C. M.; Weinhold, F. NBO Version 5. G, Theoretical Chemistry Institute, University of Wisconsin/ Madison, WI, **2004**.
[30] Nori-Shargh, D.; Mousavi, S. N.; Boggs, J. E. *J. Phys. Chem. A,* **2013**, *117*, 1621–1631.